Generation of regular optical vortex arrays using double gratings*

SUN Hai-bin (孙海滨)[1], **ZHANG Xin-yu** (张新宇)[2,3], **and SUN Ping** (孙平)[2]**
1. College of Physics and Electronic Engineering, Taishan University, Tai'an 271000, China
2. School of Physics and Electronics, Shandong Normal University, Jinan 250014, China
3. School of Physics, Beijing Institute of Technology, Beijing 100081, China

(Received 11 April 2020; Revised 16 June 2020)

In order to generate high quality regular optical vortex array (OVA), we present an experimental method for generating OVA using phase only liquid crystal spatial light modulator (LC-SLM) assisted two gratings. In the scheme, holograms of two grating are displayed on the screen of two LC-SLMs respectively; the diffraction optical fields are captured by a CCD camera. The simulated and experimental results show that the regular OVA can be generated by using double diffraction gratings. The generated OVAs have a constant topological charge of ±1. The method can provide a useful pathway to produce regular OVA for some applications in optical communication, particle trapping and optical metrology.

Document code: A **Article ID:** 1673-1905(2021)05-0317-4
DOI https://doi.org/10.1007/s11801-021-0047-0

The vortex beam is a hollow beam which has spiral phase wavefront and phase singularity. The intensity of the light wave is zero at the phase singularity, and the phase is spirally distributed around the singular point perpendicular to the propagation direction[1]. Due to these peculiar characteristics, optical vortex beams have led to many applications, such as optical trapping[2], optical tweezers[3,4], quantum information communication[5], optical communications[6,7] and optical measurement[8].

A network of optical vortices, also called optical vortex lattice or optical vortices array (OVA), has caught widespread attention owing to some distinct properties compared to isolated ones[9,10]. OVAs have been widely used in the area of optical metrology[11], the manipulation of micro-optomechanical pumps[12] and microlithography[13].

Generation of OVAs by multiple-beam interference[14], multiple-pinhole interferometer[15], lateral shearing interferometers[16], peculiar patterned metasurfaces[17], plasmonic[18], colloidal monolayers of dielectric micro-particles[19], spatial light modulator[20,21], diode-pumped microchip laser[22] and smectic liquid crystals[23] has been proposed. But most of the aforementioned interferometric techniques used for generating OVAs are based on the modified Mach-Zehnder interferometer and multiple Michelson interferometers. These experimental systems often require the use of vibration isolation table, attenuation plates, multiple beam-splitters and mirrors. This requires precise alignment of the optical components in the optical path and hence is not robust[24]. The spiral phase filtering method has higher requirements on the surface quality of the spiral phase plate, and it is difficult to process. The computational holographic method is to make high-quality holograms by optical etching, and it takes a long time to make them.

This paper proposes a method for generating regular OVAs using two gratings. In the scheme, the hologram of two grating are generated and respectively displayed on the screen of two liquid crystal spatial light modulators (LC-SLM) respectively. A laser beam is expanded, collimated and directed onto the LC-SLM screen. Simulation and experimental results are presented. The method of generating regular OVAs by double gratings' diffraction has the advantages of simple optical path structure and convenient adjustment.

Fig.1 is the schematic for generation OVAs using double gratings. The holograms of the grating A and B are respectively loaded onto the screen of SLM1 and SLM2. The laser beam is vertically incident on the screen of the LC-SLMs, and the diffraction images are captured by a CCD camera. By adjusting the distance between the two LC-SLMs and their distance from the CCD camera, a clear image can be obtained.

Fig.1 Schematic of generating OVAs using double gratings

* This work has been supported by the National Natural Science Foundation of China (Nos.61975099 and 11902317), and the Natural Science Foundation of Shandong Province of China (Nos.ZR201702090137 and ZR2017LA010).
** E-mail: sunpingmail@163.com

There are gratings A and B, and their complex amplitudes are

$g_A(x,y)=[1+\cos(mx+ny)]/2,$ (1)

$g_B(x,y)=[1+\cos(mx)]/2,$ (2)

where d is the grating stripe pitch, $m=n=2\pi/d$.

When the parallel planar light is incident perpendicularly to the grating A, the spatial spectrum is

$$G_A(f_x,f_y)=\frac{1}{2}\delta(f_x,f_y)+\frac{1}{4}[\delta(f_x-\frac{1}{d},f_y-\frac{1}{d})+\delta(f_x+\frac{1}{d},f_y+\frac{1}{d})], \quad (3)$$

where f_x and f_y are the spatial frequencies of the x-axis and y-axis on the plane after the grating, respectively. The diffracted light field is observed on the observation plane located behind the grating A, and its transfer function can be expressed as

$$H(f_x,f_y)=\exp[-j\pi\lambda z(f_x^2+f_y^2)]\cdot\exp(jkz), \quad (4)$$

where λ is the wavelength of the incident light, z is the distance between the grating A and the observation surface, $k=2\pi/\lambda$ is the wave number. The spectrum of the light field distribution at z is

$$G_A^z(f_x,f_y)=G_A(f_x,f_y)\cdot H(f_x,f_y)=\left\{\frac{1}{2}\delta(f_x,f_y)+\exp(-j\frac{2\pi\lambda z}{d^2})\cdot\frac{1}{4}[\delta(f_x-\frac{1}{d},f_y-\frac{1}{d})+\delta(f_x+\frac{1}{d},f_y+\frac{1}{d})]\right\}\exp(jkz) \ . \quad (5)$$

When the grating is illuminated by a planar wave, the diffracted field will replicate an exact image of the grating in a series of equally spaced planes. These image planes, usually called Talbot planes, are located at regular distances away from the grating. This distance is determined by

$$z_n=\frac{2nd^2}{\lambda}, \ (n=1, \ 2, \ 3...), \quad (6)$$

where d is the spatial period of the grating, λ is the wavelength of the light source, and n is a positive integer referred to as the self-image number. The first one is usually known as the Talbot distance z_T, z_{aT} and z_{bT} represent the Talbot distance of grating A and grating B, respectively.

For gratings A and B, the position of their Talbot planes are z_a and z_b.

At these Talbot planes, $\exp(-j\frac{2\pi\lambda z}{d^2})=1$, Eq.(5) becomes

$$G_A^{za}(f_x,f_y)=\left\{\frac{1}{2}\delta(f_x,f_y)+\frac{1}{4}[\delta(f_x-\frac{1}{d},f_y-\frac{1}{d})+\delta(f_x+\frac{1}{d},f_y+\frac{1}{d})]\right\}\cdot\exp(jkz_a). \quad (7)$$

The inverse Fourier transform is performed on the Eq.(7), and the complex amplitude distribution of the diffraction field of the grating A at z_a is obtained as

$$\tilde{g}_A=\frac{1}{2}\left[1+\cos(\frac{2\pi}{d}x+\frac{2\pi}{d}y)\right]\cdot\exp(jkz_a). \quad (8)$$

When the grating B is placed at a certain Talbot image plane of the grating A, the diffraction light field of the grating A is projected onto the grating B, and the diffraction field of the grating B can be expressed as

$$\tilde{g}_B=\tilde{g}_A\cdot g_B=\frac{1}{4}[2\cos(\frac{2\pi}{d}x)\cdot\cos(\frac{2\pi}{d}y)+\cos^2(\frac{2\pi}{d}x)+\cos^2(\frac{2\pi}{d}y)]\cdot\exp(jkz_a), \quad (9)$$

The spectrum at z behind the grating B is

$$G_B^z(f_x,f_y)=F(\tilde{g}_B)\cdot H(f_x,f_y). \quad (10)$$

When the diffraction distance of the gratings A and B is equal to z_{aT} and mz_{bT}, respectively, the distribution of the complex amplitude of the light field is

$$\tilde{g}_B=\frac{1}{4}[\cos(\frac{2\pi}{d}x)+\cos(\frac{2\pi}{d}y)]^2\cdot\exp[jk(z_{aT}+mz_{bT})]=\frac{1}{4}[\cos(\frac{2\pi}{d}x)+\cos(\frac{2\pi}{d}y)]^2\cdot\exp[j\frac{2d^2}{\lambda}(1+m)], \quad (11)$$

where m is a constant. Obviously, in Eq.(11), there is a vortex phase term, $\exp[j2d^2(1+m)/\lambda]=\exp(jl\varphi)$, in the formula ($l$ is the topological charge of the optical vortex). Therefore, we can conclude that there are optical vortices in the diffraction light field.

In order to further investigate the diffraction field generated by the double grating, we simulated the peak intensity of the diffraction field at different Talbot distances of the grating A at 1 time and 0.5 time of Talbot distance corresponding to the grating B, the results are shown in Fig.2. From Fig.2, we can see that the peak intensity curves corresponding to 1 time and 0.5 time of the Talbot distances of the grating B are coincide, and the grating A has the highest peak intensity at 0.58 time of Talbot distance, and the peak intensity at 1±0.06 time of Talbot distance is also higher.

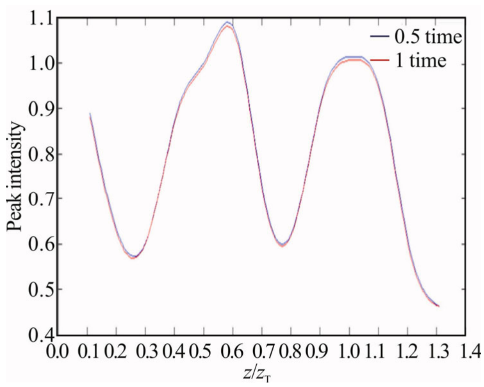

Fig.2 The curve of peak intensity of the optical vortex array at different diffraction distances of the grating A when the diffraction distance of the grating B is 1 time and 0.5 time of Talbot distance

In the numerical simulation, the distance between gratings A and B is z_T, and the diffraction distance of the grating B is $0.5z_T$. When the duty cycles of the designed gratings A and B are 63% and 52% respectively, the duty cycle of the generated OVAs is 60%. When the duty cycles of the gratings A and B are 55% and 52% respectively, the duty cycle of the OVAs is reduced to 10%.

We built the optical system schematically shown in Fig.3 to test our method. He-Ne laser is with the wavelength of 632.8 nm. The laser beam passes through an attenuating sheet (A), a beam expanding mirror (E), a spatial filter (S), and a collimating lens (L) in sequence. Thereafter, the SLM1 and SLM2 are irradiated vertically, and a CCD camera was placed at a certain distance after the SLM2 to capture the intensity profile of resultant wave-field. The LC-SLM used in our experiment was phase-only modulator with 1 920×1 080 pixels, and each pixel had dimensions of 8.5 μm×8.5 μm (HDSLM85T). The diffraction efficiency of the LC-SLM is 60%. The CCD camera was an image sensor with 768×576 pixels at 8-bit resolution. The distance between the SLM1 and the SLM2 is z_1, and the distance between the SLM2 and the CCD is z_2.

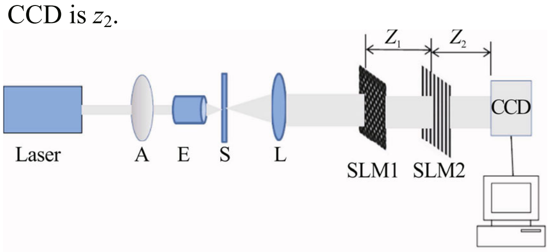

Fig.3 System of generating OVA using double gratings to test our method

We designed the hologram of the gratings using Matlab. The sizes of the gratings A and B are 512×512 pixels, $m=n=2\pi/d$, d=100 μm, as shown in Fig.4. The duty cycles of the gratings A and B are 63% and 52% respectively. The numerically computed gratings A and B were electronically displayed on the screen of SLM1 and SLM2, respectively. In the experiments, the wavelength of the incident beam is 632.8 nm, and the Talbot distance z_T is 15.8 mm. The experimental results are shown in Fig.5. In the experiments, z_1=1.1, z_T=17.388 mm, z_2=15.8 mm, 7.9 mm, 3.95 mm, respectively. Fig.5(a1), (a2), (a3) are the simulation results and Fig.5(b1), (b2), (b3) are the experimental results. The size of these images is 512×512 pixels. In the experiments, the distance between the grating A and the grating B is $1.1z_T$. Considering the experimental error, this distance value is basically consistent with the theoretical calculation value. The duty cycles of the generated OVAs are 53%, 62% and 60% respectively, which is in good agreement with the theoretical value.

In order to confirm the existence of the optical vortices, we displayed the output optical field's pattern of OVA on the screen of LC-SLM, and superimposed the output beam with a titled planar wave. The interference pattern is shown in Fig.6. Fig.6(a) is the simulation result; (b) is the experimental result, and (c) is an enlargement of the blue rectangular area in (b). The interference patterns (circled in yellow) in the figure appear bifurcated, which confirm the existence of the optical vortices in the OVAs. The divergence directions of the patterns are opposite for the +1 and −1 defects, that is, the topological charge of the optical vortices in the OVAs is ±1. These experimental results confirm the simulation results. The simulation results accord well with the experimental results.

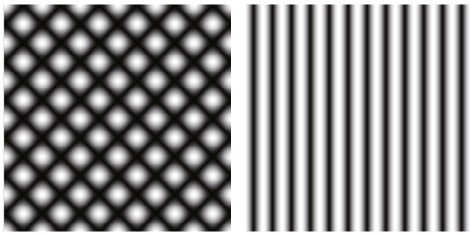

(a) Grating A (b) Grating B

Fig.4 Gratings used in the experiment

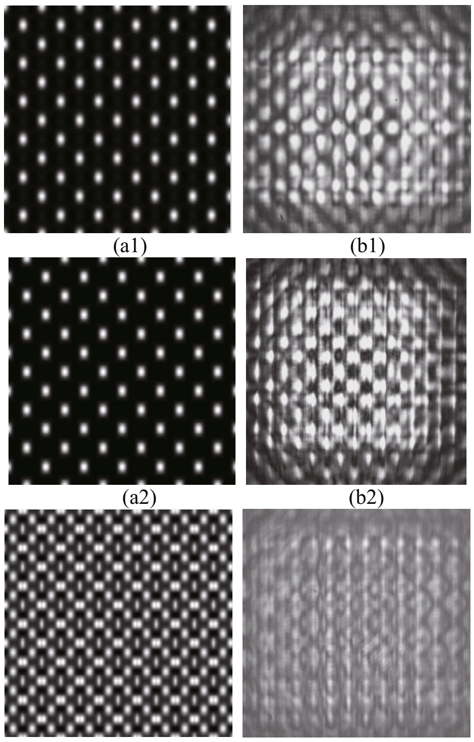

(a1) (b1) (a2) (b2) (a3) (b3)

Fig.5 Experimental results: (a1), (a2), (a3) Simulation results; (b1), (b2), (b3) Experimental results

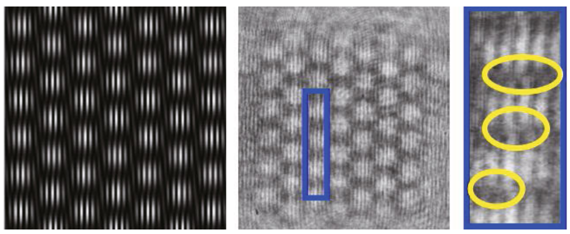

(a) (b) (c)

Fig.6 Confirmation of OVA: (a) Simulated result; (b) and (c) Experimental results

Fig.7 shows the phase map of the OVA. Fig.7(a) is the simulation result when the diffraction distance is 750 mm, (b) and (c) are the experimental results when the diffraction distance is 750 mm and 900 mm respectively. The experimental results demonstrated that the phase of the OVA also changes when the diffraction distance changes.

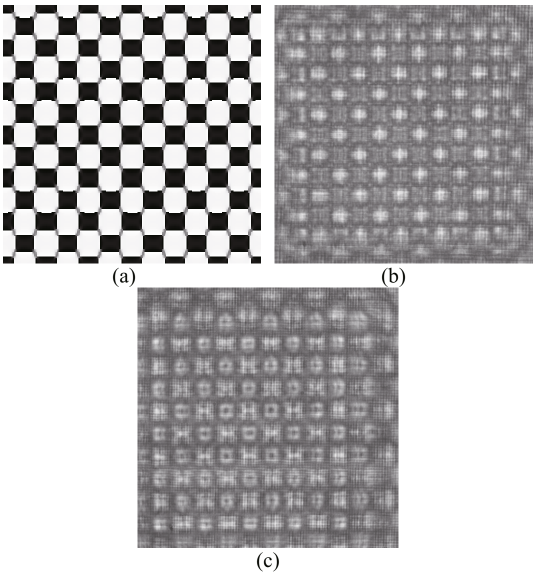

Fig.7 Phase maps of the OVA: (a) Simulation result; (b) and (c) Experimental results

In conclusion, we have demonstrated a simple experimental method for generating regular OVA with a topological charge of ±1 by making use of phase only LC-SLM assisted two gratings. The holograms of two gratings are displayed on the screen of two LC-SLMs. Simulation and experimental results are presented. The results show that OVA has good regularity when the diffraction distance of the grating B is one-half and one-times of the Talbot distance of the grating B. The method for generating regular OVA by double gratings diffraction has the advantages of simple optical path structure and convenient adjustment. The present system has potential applications in optical communication, particle trapping and optical metrology.

References

[1] Wang Han, Liu Lixia, Zhou Changda, Xu Jilian, Zhang Meina, Teng Shuyun and Cai Yangjian, Nanophotonics **8**, 317 (2019).

[2] Favre-Bulle Itia A., Stilgoe Alexander B., Scott Ethan K. and Rubinsztein-Dunlop Halina, Nanophotonics **8**, 1023 (2019).

[3] Ranha Neves Antonio Alvaro and Cesar Carlos Lenz, Journal of the Optical Society of America B **36**, 1525 (2019).

[4] Baudoin Michael, Gerbedoen Jean-Claude, Riaud Antoine, Matar Olivier Bou, Smagin Nikolay and Thomas Jean-Louis, Science Advances **5**, eaav1967 (2019).

[5] Flamini Fulvio, Spagnolo Nicolò and Sciarrino Fabio, Reports on Progress in Physics **82**, 016001 (2019).

[6] Zou Li, Gu Xiaofan and Wang Le, Optics Communications **410**, 333 (2018).

[7] Gong Lei, Zhao Qian, Zhang Hao, Hu XinYao, Huang Kun, Yang JiaMiao and Li YinMei, Light: Science & Applications **8**, 27 (2019).

[8] Zhang Xinyu, Hu Chunhua and Sun Ping, Optik **185**, 1071 (2019).

[9] Wang Xuewen, Nie Zhongquan, Liang Yao, Wang Jian, Li Tao and Jia Baohua, Nanophotonics 7, 1533 (2018).

[10] Song Limin, Yang Zhenjun, Zhang Shumin and Li Xingliang, Physical Review A **99**, 063817 (2019).

[11] Senthilkumaran P., Masajada Jan and Sato Shunichi, International Journal of Optics **2012**, 1 (2012).

[12] Ladavac Kosta and Grier David, Optics Express **12**, 1144 (2004).

[13] Yashiki Satoshi, Applied Optics **54**, 5353 (2015).

[14] Liu Kunpeng, Liu Zhigang and Dong Xiaochun, Optics Express **27**, 21652 (2019).

[15] Jiang Shuna, Li Xing, Ma Li, Gao Yaru, Gui Weiling and Cheng Chuanfu, Chinese Physics Letters **32**, 104209 (2015).

[16] Ghai Devinder Pal, Vyas Sunil, Senthilkumaran P. and Sirohi R. S., Optics Communications **282**, 2692 (2009).

[17] Lin Zemeng, Li Xiaowei, Zhao Ruizhe, Song Xu, Wang Yongtian and Huang Lingling, Nanophotonics **8**, 1079 (2019).

[18] Wang Yu, Xu Yuntao, Feng Xue, Zhao Peng, Liu Fang, Cui Kaiyu, Zhang Wei and Huang Yidong, Optics Letters **41**, 1478 (2016).

[19] Mitin Nikolai and Pikulin Alexander, Optics Letters **42**, 2527 (2017).

[20] Huang T. D. and Lu T. H., Optics Letters **44**, 3917 (2019).

[21] Wang Y. K., Ma H. X., Zhu L. H., Tai Y. P. and Li X. Z., Applied Physics Letters **116**, 011101 (2020).

[22] Chen Dimeng, Miao Yujie, Wang Hanjie and Dong Jun, Journal of Physics: Photonics **2**, 035002 (2020).

[23] Feng Fu, Wei ShiBiao, Li Ling, Min ChangJun and Somekh Michael, Optics Express **27**, 27536 (2019).

[24] Singh Brijesh Kumar, Singh G., Senthilkumaran P. and Mehta D. S., International Journal of Optics **2012**, 7 (2012).